Ion Beam "Photography": Decoupling Nucleation and Growth of Metal Clusters in Glass

E. Valentin,[1,2] H. Bernas,[1,*] C. Ricolleau,[3] and F. Creuzet[4]

[1]*Centre de Spectrométrie Nucléaire et de Spectrométrie de Masse, 91405-Orsay, France*
[2]*Laboratoire CNRS/Saint-Gobain, 93303-Aubervilliers, France*
[3]*Laboratoire de Minéralogie et de Cristallographie de Paris, 75252-Paris, France*
[4]*Fontainebleau Research Center, Corning S.A., 77210-Avon, France*

(Received 3 March 2000; revised manuscript received 31 August 2000)

We demonstrate that room temperature MeV ion irradiation of a glass containing copper oxide initiates nucleation of pure Cu clusters via the inelastic "electronic" component of the ion energy loss, when the latter is above a threshold value. The clusters grow under subsequent thermal annealing, following Lifshitz-Slyozov-Wagner kinetics. The decoupling of nucleation and growth is analogous to that occurring in the photographic process. It allows total control over the cluster density, average size, and size distribution.

DOI: 10.1103/PhysRevLett.86.99 PACS numbers: 61.80.Jh, 61.46.+w, 61.72.Qq, 79.20.Rf

The study of atomic cluster properties [1] usually requires that they be trapped in an adequate environment. Glasses containing metallic nanoclusters [2] are attractive candidates for experiments in which minimal chemical interaction is required between the cluster and its host, thus allowing optical studies of such basic nanocluster properties as the large third-order susceptibility, second harmonic generation and picosecond response time [2–4], as well as suggesting interesting applications in optical switching and/or filtering. Individual properties of magnetic clusters and their interactions [5] may also be studied in this way. Controlling the size distribution and the density of clusters has been successful only in a few instances, notably via specific sol-gel techniques [6]. Forcing solute supersaturation inside the glass (via cosputtering, sol-gel methods, ion implantation, or irradiation) and then annealing at a temperature where diffusion can occur leads to clusters that nucleate (and hence grow) at different times. Subsequent precipitate population evolution (so-called Ostwald ripening) then leads to broad size distributions, with little control over the average cluster size and density. We report an MeV ion irradiation technique which allows us to (i) bias the cluster formation chemistry, producing only metal clusters, and (ii) decouple the nucleation and growth processes entirely. Nucleation is shown to require a threshold in the energy deposited into electron motion in the glass. The nucleation probability (hence the cluster density) is modeled very simply. All the clusters grow simultaneously under postirradiation thermal annealing, minimizing their size distribution. The latter follows the Lifshitz-Slyozov-Wagner (LSW) theory [7] of diffusion-limited precipitate ripening. Complete control over the density, the average size (from 2 to 8 nm), and the size distribution (FWHM typically 2 nm) of Cu metal clusters was thus obtained in an SiO_2-based glass.

In previous metal cluster syntheses involving ion implantation (e.g., Refs. [2–5]), the metal atoms implanted into the glass did not interact with the host. Chemical potential gradients favored metal clustering during high temperature annealing, and the damage — which was produced mostly by collisional (so-called nuclear S_n) ion stopping processes — was eliminated by the anneal. An alternative approach involved irradiating a glass containing a metal oxide (typically at the 1%–10% concentration level) with very high fluences of protons or He ions at energies between about 0.1 and 1.5 MeV (Refs. [2] and [8]). Nanocluster precipitation then occurred during irradiation via the inelastic energy transferred to the electrons (the so-called electronic energy loss S_e), an effect ascribed to interactions between the metal and irradiation-induced defects. Both methods provide some control over the cluster density via the ion fluence, but neither can bias the nucleation and growth processes. Our approach also involves electronic stopping in glasses, but with two major differences: We use MeV heavy ion irradiations with far larger energy depositions, and as a consequence of the very low fluences which are then required, a simple relation may be established between the nucleation probability and the statistics of individual ion impacts.

Samples were Cu oxide-containing glasses (composition by wt % approximately 74 SiO_2, 16 Na_2O, 8 CaO, 0.11 SnO_2, 0.08 Cu_2O). The structural identification of the clusters, as well as size and depth distribution measurements, was performed by plane view and cross-sectional high resolution electron microscopy (HREM) using a 200 kV Topcon EM002-B or a 200 kV Hitachi 9000 FEG electron microscope with lattice resolutions of, respectively, 0.18 nm and 0.20 nm. Lattice images were digitized with a CCD video camera and analyzed using standard Fourier transform procedures. Some density and depth measurements were performed with a 120 kV Philips CM12 transmission electron microscopy. Samples were prepared via the tripod technique or by low-angle Ar ion polishing. A prior study [9] of cluster formation in the same glasses by thermal annealing alone showed that visible clusters appeared only at annealing temperatures above 853 K. We then found a bimodal size distribution (not shown here) whose mean sizes (initially around 5 nm

and 8 nm, respectively) increased with the annealing time. HREM observations showed that *both* Cu_2O and pure Cu clusters [identified by the (111) Cu_2O interplane distance at 0.246 nm and the (111) Cu interplane distance at 0.208 nm] occurred in the entire size range.

The effect of MeV ion irradiation on cluster formation is strikingly different. Room temperature irradiations were performed on the ARAMIS accelerator [10] with 11.9 MeV Br, 7 MeV Si, or 6 MeV O ions at fluences ranging from 5×10^{11} to 5×10^{13} ions cm^{-2}. The ion beam flux was below 2×10^{11} ions $cm^{-2}\,s^{-1}$ to limit sample heating to a few degrees. Ion energy loss parameters were calculated using the SRIM98 code [11]. No clusters were visible after room temperature irradiation alone. Postirradiation anneals at 673 K (well below the formation threshold in purely thermal treatments) were performed for at least 600 s in order to obtain complete cluster size distributions, i.e., such that their minimum size was above the visibility threshold of our HREM conditions.

Our main experimental results are the following. First, ion irradiation biases the chemistry of cluster formation: (111) lattice plane measurements revealed that only pure Cu metal particles were formed. Second, cluster nucleation is essentially (or solely) due to electronic stopping. Below a depleted zone 100 nm under the surface (ascribed to glass hydration leading to Cu outdiffusion [12]), cross-sectional HREM showed that nanocluster formation occurred only (Fig. 1) in the first 40% of the ion stopping region (the ion penetration depth was $\sim 4\ \mu$m for all our ion mass-and-energy combinations). Within this depth range, the cluster formation probability depends on the electronic component S_e of the ion energy loss (full line in Fig. 1) which is 5–100 times larger than S_n in our irradiations. No clusters are formed towards the end of the ion range, where S_n increases. Varying the ratio S_e/S_n by changing the irradiating ion mass and energy confirmed this conclusion. The effect of S_n on cluster formation is hence small or nil in these experiments, particularly since clusters were formed in a range of ion fluences (10^{11}–10^{13} ions cm^{-2}) where collisional ion beam mixing and redissolution are negligible. The Fig. 1 inset shows the cluster size distribution obtained in this way.

Figure 1 suggests the existence of a threshold S_e value for cluster nucleation. Irradiating with 7 MeV Si (S_e = 3.2 keV/nm) or 6 MeV O (S_e = 1.9 keV/nm) ions led to cluster formation curves parallel to the one shown in Fig. 1 for 11.9 MeV Br (S_e = 4.1 keV/nm); i.e., the irradiation and subsequent annealing treatment described above led to cluster formation down to a maximum depth that depended on the ion's S_e value. After irradiating with 11.9 MeV Br or 7 MeV Si ions at a fluence of 10^{13} ions cm^{-2}, cluster formation required an *apparent* threshold of 2.5 keV/nm. When irradiating with 6 MeV O ions, the apparent threshold was 1.65 keV/nm, but the near-surface cluster density then saturated only at fluences that were some 10 times

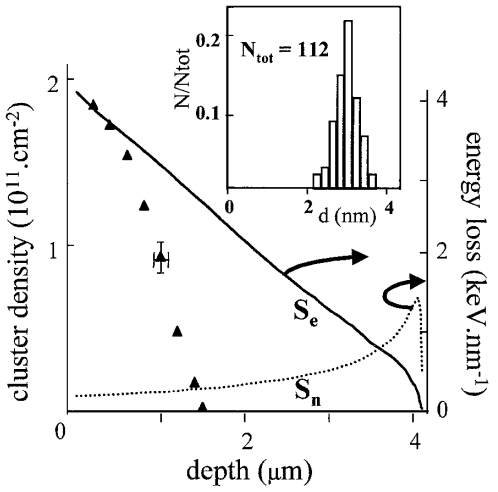

FIG. 1. Depth dependence of the pure Cu cluster density (triangles, left axis) after irradiation of the Cu_2O-containing glass with 11.9 MeV Br at a fluence of 10^{13} ions cm^{-2}, compared to the electronic (full curve) and nuclear (dotted curve) components [11] of the Br ion energy loss (right axis). Postrirradiation annealing was performed at 673 K for 600 s (see text). The inset shows the Cu cluster size distribution (diameter d) corresponding to the first data point.

higher. Thus, using different ion mass-energy combinations, the cluster depth distribution scaled with the energy deposited in electronic stopping, but cluster formation also depended on the irradiating ion fluence. This suggested the following analysis of MeV ion-induced cluster nucleation.

The energy deposited into electron motion by an incoming ion is not continuous but is actually a statistical variable. We divide the sample into elementary volumes and assume that *separate, additive electronic energy depositions* inside such a volume may induce Cu cluster nucleation. Depending on the ion-energy combination involved, the cluster formation probability then depends on the number of energy deposition increments inside the elementary volume. Each experimental point in Fig. 1 corresponds to a 100 nm thick slice. Consider the first of these, with maximum cluster density: The average distance between clusters is above $\approx$60 nm, so that on average this slice thickness accommodates at most just one cluster. We may thus replace the elementary volume by its projected surface σ in order to calculate the fluence dependence of the areal cluster density in this slice.

Figure 2 compares the experimental areal cluster densities as defined above with those deduced from the probability

$$\sum_{n_c}^{\infty} P_n = \sum_{n_c}^{\infty} [(\sigma F)^n / n!] e^{-(\sigma F)} \qquad (1)$$

of having more than n_c increments of deposited energy on the surface σ (full curves). F is the ion fluence per cm^2. For Br (11.9 MeV) irradiation (full triangles), $n_c = 2$ increments within σ are required for nucleation to occur. For

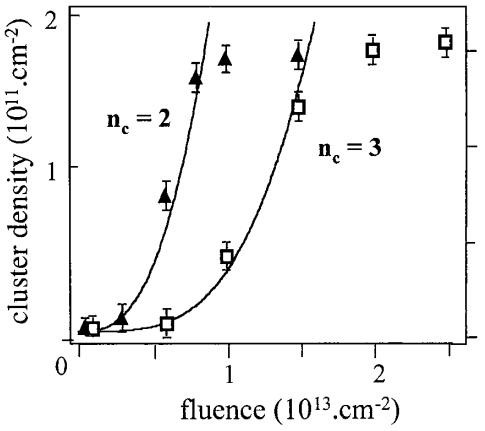

FIG. 2. Ion fluence dependence of the Cu cluster areal density for the 100 nm thick layer corresponding to the first (near-surface) data point in Fig. 1. Results are for 11.9 MeV Br (full triangles) and 6 MeV O (Open squares) irradiations. The curves are $F \times (\sum P_n)$, where F is the ion fluence and $(\sum P_n)$ is from Eq. (1) (see text). Both data sets are fitted independently assuming that the radius of σ is 1 nm. Experimental densities saturate when the entire Cu content in the layer has clustered.

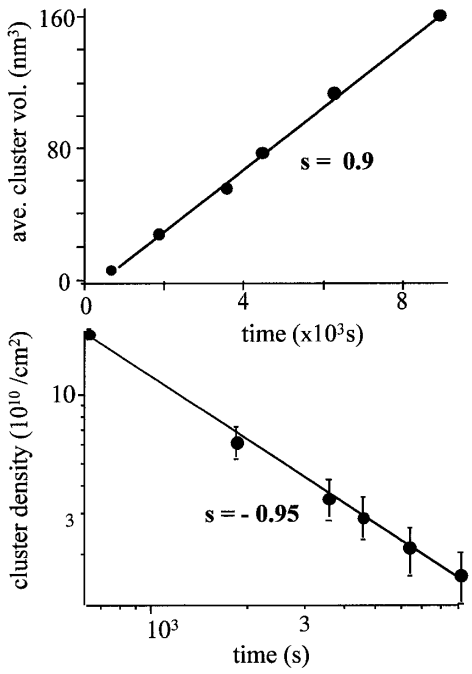

FIG. 3. Time evolution of average volume (upper part) and density (lower part) of Cu clusters under thermal annealing at 673 K, after nucleation by 11.9 MeV Br irradiation (fluence 10^{13} ions cm^{-2}). Scales of upper figure are linear; those below are logarithmic. The slope of both lines is very close to unity, as expected from Ref. [7] (note that their definitions are different).

O (6 MeV) irradiation (open squares), $n_c = 3$ increments are required. The parameter needed to fit each curve is the surface σ, whose radius r is found to be $r \approx 1$ nm in both cases. For cluster nucleation to occur, the average deposited energy must exceed $2 \times (2.5$ keV/nm) for the Br irradiation and $3 \times (1.65$ keV/nm) for the O irradiation; i.e., there is a unique "threshold" (5.0 keV/nm) for nucleation, which may be reached in independent increments. We confirmed that nucleation could occur for $n_c = 1$ by performing [9] the same experiment with 580 MeV Ag ions (for which $S_e = 13$ keV/nm) delivered by the GANIL accelerator (Caen, France). The saturation effect observed in Fig. 2 occurs when all the Cu atoms in the slice have clustered. This was checked [9] on glasses with two different Cu_2O concentrations (0.08 and 0.16 wt %). Note that the same calculation allows us to estimate the cluster density deeper in the sample; the only difference is an increase in n_c as S_e is reduced along the ion path. The present cluster formation mechanism differs considerably from those described previously, since nucleation occurs at fluences low enough to reveal that the energy deposited along the individual ion track is a relevant parameter.

The cluster growth kinetics were determined by transmission electron microscopy and HREM studies after postirradiation annealing (at 673 K) at increasing times (Fig. 3). In agreement with the LSW theory [7] of diffusion-limited precipitate evolution, we find an inverse time dependence of the cluster density, and $r^3 - r_0^3 \approx st$, where r is the cluster radius (r_0 is the particle radius at time zero) and t is the time during which the particles grow under irradiation-induced diffusion. In a forthcoming publication (see also [9]), we will show that (i) our cluster size distributions after long-term annealing display the characteristic universal shape predicted in Ref. [7] and (ii) identical results are obtained in experiments involving glasses without reducing components or glasses containing NiO rather than Cu_2O.

The analysis given above predicts the irradiation-induced cluster densities but says little about the nucleation mechanism. Pure Cu from the oxide dissolved in the glass can only precipitate if (i) the Cu ionization state is changed, since Cu^0 is the sole diffusing species [13], and (ii) Cu^0 stability (for hours, at least) is compatible with overall charge equilibrium in the glass. Cu neutralization may be produced in the glass by the very high secondary electron recoil density accompanying the stopping MeV ion [14]. The average range of these electrons (extrapolated from the results of Ref. [15]) is roughly 15 nm, in agreement with the Cu capture radius for cluster formation deduced from the fluence values for which cluster density saturation occurs in Fig. 2. The stabilization of Cu^0 may occur via irradiation-induced defects that trap positive charges and/or by interaction with the hydrogen impurities that abound in a glass [16]. Recoil electron-induced neutralization is thus a plausible source of Cu mobility upon low temperature annealing. The existence of an energy deposition threshold then finds a natural explanation: The number of Cu atoms which are neutralized (and hence diffuse) inside a volume of radius r must be sufficient to form a stable cluster nucleus; i.e., it is the nucleation volume. The threshold is reachable in separate additive steps because the newly

formed Cu^0 atoms cannot diffuse at room temperature, the 673 K anneal being required for clustering to set in. The $\approx$15 nm capture radius deduced from Fig. 2 determines the clusters' growth volume.

MeV ion irradiation thus triggers nucleation of pure metal clusters in a glass containing the metal oxide and allows control over their density. An independent thermal annealing stage provides control (via LSW growth) over the cluster size distribution. The analogy with the photographic process is rather striking. Understanding how far it may be carried requires further scrutiny of the relation between the energy deposition mechanism and metal precipitation. Combined with appropriate masking techniques, this method could find interesting applications (notably in optoelectronics and magnetism), especially if the initial metal concentration may be significantly increased. Recent results indicate that this is the case.

We thank M. O. Ruault, O. Kaitasov, and C. Pélissié for their contributions, M. Hÿtch, J. Devaud, and M. Lancin for help in using their HREM facilities, and E. Balanzat for help with the GANIL irradiation. Discussions with V. A. Borodin, K.-H. Heinig, G. Petite, and A. M. Stoneham are gratefully acknowledged. CSNSM is UMR CNRS-IN2P3–Université Paris-Sud; LMCP is UMR CNRS-Universités Paris 6-7.

*Electronic address: bernas@csnsm.in2p3.fr

[1] U. Kreibig and M. Vollmer, *Optical Properties of Metal Clusters* (Springer-Verlag, Berlin, New York, 1995).

[2] For example, R. Haglund, Jr., Li Yang, R. H. Magruder III, C. W. White, R. A. Zuhr, Lina Yang, R. Dorsinville, and R. R. Alfano, Nucl. Instrum. Methods Phys. Res., Sect. B **91**, 493 (1994).

[3] G. De Marchi, F. Gonella, P. Mazzoldi, G. Battaglin, E. J. Knystautas, and C. Meneghini, J. Non-Cryst. Solids **196**, 79 (1996); F. Hache, D. Ricard, C. Flytzanis, and U. Kreibig, Appl. Phys. A **47**, 347 (1988).

[4] P. Mazzoldi, G. W. Arnold, G. Battaglin, R. Bertoncello, and F. Gonella, Nucl. Instrum. Methods Phys. Res., Sect. B **91**, 478 (1994).

[5] D. L. Leslie-Pelecky and R. B. Rieke, Chem. Mater. **8**, 1770 (1996); T. Isobe, R. A. Weeks, and R. A. Zuhr, Solid State Commun. **105**, 469 (1998).

[6] For a recent example, see N. Feltin, L. Levy, D. Ingert, E. Vincent, and M. P. Pileni, J. Appl. Phys. **87**, 1415 (2000).

[7] I. M. Lifshitz and V. V. Slyozov, J. Phys. Chem. Solids **19**, 35 (1961); C. Wagner, Z. Elektrochem. **65**, 581 (1961).

[8] H. Hosono, N. Matsunami, A. Kudo, and T. Ohtsuka, Appl. Phys. Lett. **65**, 1632 (1994); H. Hosono *et al.,* J. Appl. Phys. **82**, 4232 (1997), and references therein.

[9] E. Valentin, Ph.D. thesis, Ecole Centrale de Paris, 1999; also E. Valentin, H. Bernas, C. Ricolleau, F. Creuzet, and E. Balanzat (unpublished).

[10] H. Bernas, J. Chaumont, E. Cottereau, R. Meunier, A. Traverse, C. Clerc, O. Kaitasov, F. Lalu, D. Ledu, G. Moroy, and M. Salomé, Nucl. Instrum. Methods Phys. Res., Sect. B **62**, 416 (1992).

[11] J. F. Ziegler, J. P. Biersack, and U. Littmark, *The Stopping and Range of Ions in Solids* (Pergamon, New York, 1985); http://www.research.ibm.com/ionbeams/SRIM/

[12] G. W. Arnold, G. De Marchi, P. Mazzoldi, and G. Battaglin, Nucl. Instrum. Methods Phys. Res., Sect. B **116**, 364 (1996).

[13] W. A. Hayes and A. M. Stoneham, *Defects and Defect Processes in Non-Metallic Solids* (Wiley, New York, 1985), p. 317 et seq.

[14] B. Boizot, G. Petite, D. Ghaleb, and G. Calas, Nucl. Instrum. Methods Phys. Res., Sect. B **141**, 580 (1998).

[15] M. Toulemonde, C. Dufour, and E. Paumier, Phys. Rev. B **46**, 14 362 (1992).

[16] We thank A. M. Stoneham for drawing our attention to this point.